

See discussions, stats, and author profiles for this publication at: <https://www.researchgate.net/publication/49293218>

Formation of Stable Mesoglobules by a Thermosensitive Dendronized Polymer

ARTICLE in *MACROMOLECULES* · SEPTEMBER 2009

Impact Factor: 5.8 · DOI: 10.1021/ma901135a · Source: OAI

CITATIONS

27

READS

26

7 AUTHORS, INCLUDING:



Frank Polzer

Humboldt-Universität zu Berlin

40 PUBLICATIONS 1,068 CITATIONS

[SEE PROFILE](#)



Matthias Ballauff

Helmholtz-Zentrum Berlin

434 PUBLICATIONS 13,633 CITATIONS

[SEE PROFILE](#)



Wen li

Shanghai University

37 PUBLICATIONS 730 CITATIONS

[SEE PROFILE](#)



Afang Zhang

Shanghai University

77 PUBLICATIONS 1,579 CITATIONS

[SEE PROFILE](#)

Formation of Stable Mesoglobules by a Thermosensitive Dendronized Polymer

Sreenath Bolisetty, Christian Schneider, Frank Polzer, and Matthias Ballauff^{*,†}

Physikalische Chemie I, University of Bayreuth, 95440 Bayreuth, Germany

Wen Li, Afang Zhang,^{*} and A. Dieter Schlüter

Institute of Polymers, Department of Materials, ETH Zürich, Wolfgang-Pauli-Strasse 10, HCI G 525, 8093 Zurich, Switzerland [†]*Present address: Soft Matter and Functional Materials, Helmholtz-Zentrum Berlin für Materialien und Energie GmbH, Glienicker Strasse 100, 14109 Berlin, Germany, and Department of Physics, Humboldt University Berlin, Newtonstr. 15, 12489 Berlin, Germany.*

Received May 25, 2009; Revised Manuscript Received August 11, 2009

ABSTRACT: We present a study on the formation of stable mesoglobules by a thermosensitive dendronized polymer in aqueous solution. The polymer consists of a polymethacrylate backbone ($M_n = 0.34 \times 10^6$, $M_w = 1.1 \times 10^6$ g/mol) with ethoxy-terminated oligoethylene oxide (OEO) dendrons of second generation appended onto each repeat unit. The collapse of the dendronized chains as well as their aggregation with increasing temperature is followed by monitoring the hydrodynamic radius R_h as a function of temperature with dynamic light scattering. The aggregation of the polymer stops at a certain size that depends on the heating rate leading to the formation of stable mesoglobules. Cryogenic transmission electron microscopy demonstrates that these mesoglobules adopt a spherical shape and are rather monodisperse. It is found that for dilute concentrations the size of the mesoglobules at 50 °C only weakly depends on concentration. Moreover, no hysteresis of the formation of mesoglobules is found; that is, R_h is solely a function of temperature for both heating and cooling runs. The kinetics of the early stage of mesoglobule formation can be monitored by measurements of R_h as the function of time. It can be modeled in terms of diffusion-limited colloid aggregation (DLCA). The transition from the DLCA to the stable mesoglobules is found to be well-defined. Different possible origins of the stability that prevents further aggregation are discussed. A weak electrostatic stabilization caused by charges that are complexed by the OEO dendrons is the primary reason for the marked transition from the DLCA to the stable mesoglobules. Most probably, an additional slowing down of the coalescence of the mesoglobules is effected by vitrification.

Introduction

Phase separation of polymers in poor solvents is among the classical subjects of polymer science.¹ Homopolymers dissolved in a poor solvent will undergo phase separation below the θ -temperature, leading to the formation of macroscopic phases. In an early stage of this process, the polymer chains will associate and form larger and larger globular structures. The process of association will continue until all globules have been associated to form a macroscopic phase. However, copolymers composed of hydrophilic repeat units together with a certain percentage of hydrophobic units can associate to an intermediate state termed mesoglobule.^{2,3} The resulting micelle-like structures have been intensively studied in the past years.^{4–7} The more hydrophilic parts are located preferably at the periphery of the mesoglobule, thus providing sufficient steric stabilization. The more hydrophobic parts are buried inside of the globule, and the formation of mesoglobules can be compared with the folding transition of globular proteins.⁸ Up to now, light scattering,^{9–11} differential scanning calorimetry,¹² fluorescence spectroscopy^{13,14} and turbidity studies¹⁵ have been successfully used as analytical tools to follow the process of mesoglobule formation. The kinetics of the globule formation is fairly well understood in terms of

analytical theory¹⁶ and by Monte Carlo simulation.¹⁷ Thus, a multistage process for mesoglobule formation¹⁸ subdivided into nuclei formation, growth of the nuclei into clusters, and cluster–cluster aggregation has been proposed to explain the formation of mesoglobules.¹⁶ Using a stopped flow device and fluorescence,¹⁹ Liu et al. successfully identified the different stages during the formation of mesoglobules as proposed by theory. The influence of temperature on the formation of mesoglobules was investigated in these experiments as well.^{19,20}

Recently, we demonstrated that the thermoresponsive dendronized polymer **PG2** (Figure 1) undergoes a sharp, fast and fully reversible phase transition in aqueous solution at 36 °C.²¹ Moreover, it was shown by optical microscopy that this transition leads to the formation of globular structures. However, given the techniques used in this study, only the later stage of the mesoglobule formation could be studied. Here we present the study of the early stage of the coil-to-globule transition of dilute solutions of **PG2**. Using dynamic light scattering (DLS), we demonstrate that the association of the **PG2** in aqueous solution leads to well-defined and stable mesoglobules. Special attention is paid to the transition from the early stage in which the dendronized polymer coagulates to the final stage in which stable mesoglobules are suspended in the solution. Thus, the kinetics of aggregation in the early stage is analyzed using dynamic light scattering. The formation of mesoglobules can be monitored with great precision by following their hydrodynamic radius as a function of time.

^{*}Corresponding authors. E-mail: matthias.ballauff@helmholtz-berlin.de (M.B.); afang.zhang@mat.ethz.ch (A.F.).

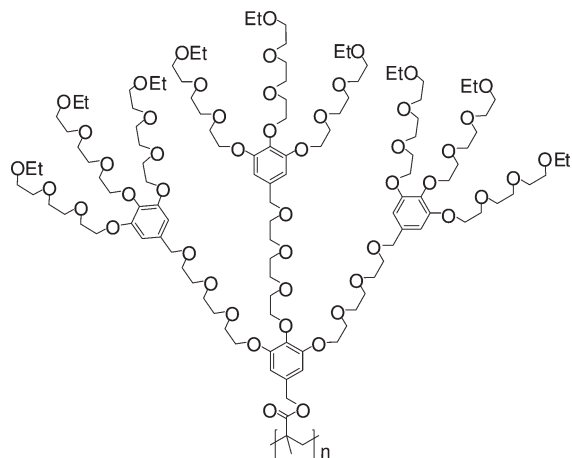


Figure 1. Chemical structure of ethoxy-terminated dendronized poly(methacrylate) **PG2**. The polymer's lateral substituent has two consecutive branching points (second generation, G2).

These data can be modeled using the theory of Wagner and co-workers.²² The result of this evaluation allows us to distinguish between the different states of the formation of mesoglobules. Moreover, the polymer in solution as well as the resulting mesoglobules are visualized by cryogenic transmission electron microscopy (cryo-TEM)²³ which allows us to study systems in situ, that is, directly in solution.

Experimental Section

Materials. The details of the synthesis of **PG2** can be found in ref 21. The molecular weight of the sample used here was $M_n = 0.34 \times 10^6$, $M_w = 1.1 \times 10^6$ g/mol.

Cryo-Transmission Electron Microscopy. Initially, the stock solution contained 0.01 wt % of dissolved dendronized poly(methacrylate) and was kept at constant temperatures of 25 and 60 °C using a water bath controlled by a thermostat. For the cryosample preparation at a temperature of 60 °C, the chamber was kept at 60 °C and vitrified rapidly by the method described in ref 23. The samples were prepared by adding a 2 μ L solution droplet on a TEM lacey carbon copper grid (200 mesh, Science Services, Munich, Germany) and removing most of the liquid with blotting paper, thus leaving a thin film stretched over the lace. The specimens were prepared by verification of thin liquid films of the desired temperature in liquid ethane at its freezing point to ~ 77 K in a temperature-controlled freezing unit (Zeiss cryo box, Zeiss NTS GmbH, Oberkochen, Germany). After freezing, the specimen was placed into a cryo-transfer holder (CT 3500, Gatan, München, Germany) and transferred to a Zeiss 922 OMEGA EFTEM (Zeiss NTS GmbH, Oberkochen, Germany). The TEM was operated at an acceleration voltage of 200 kV. Zero-loss filtered images were taken under reduced dose conditions (500–2000 e/nm²). All images were recorded digitally by a bottom-mounted CCD camera system (UltraScan 1000, Gatan, Munich, Germany) and processed with a digital imaging processing system (Digital Micrograph 3.9 for GMS 1.4, Gatan, Muenchen, Germany).

Light Scattering. The static and dynamic light scattering experiments were carried out by using the ALV/DLS/SLS-5000 compact goniometer system with a multiple tau digital correlator system, equipped with a He–Ne laser ($\lambda = 632.8$ nm). The temperature of the sample cell was maintained exactly by using a program-controlled thermostat within the error of 0.1 °C. The solutions were filtered into dust-free optical cells using 0.2 μ m nylon syringe filters. The normalized intensity correlation functions were evaluated using the CONTIN 2DP program. The hydrodynamic radius of the thermosensitive dendronized polymer was calculated using the Stokes–Einstein relation at the corresponding temperature. Measurements of the

time-resolved aggregation kinetics were performed at a scattering angle of 90° at regular interval of 10 s.

Modeling of the Data

In order to follow the aggregation in a quantitative manner, we measured the hydrodynamic radius R_h of the aggregates as a function of time. This procedure leads directly to the rate constant of binary collisions between the dissolved polymers if the concentration is low enough.²⁴ Thus, Borkovec and co-workers were able to study the rate of doublet formation of latex particles with great precision.^{25,26} However, it was found that the process of aggregation is much too fast for the present system to be able to attain the regime in which aggregation has not proceeded much beyond the stage of dimerization. Dilution of the solution is not possible since it would reduce the scattering intensity of the system too much. Hence, the approach devised by Wagner and co-workers²² was used which is valid at a later time as well. It is based on earlier work by Lin and colleagues that considers the aggregation of spherical colloids in dilute suspension.^{27–29} In short, two limiting cases must be considered: The diffusion-limited colloid aggregation (DLCA) occurs when the particles have no repulsive interaction. Moreover, it is assumed that aggregation is irreversible. In the reaction-limited colloidal aggregation (RLCA) the particles have a weak but finite repulsive interaction that may be overcome by Brownian motion. In both cases, the aggregates have a fractal structure characterized by a fractal dimension d_f of the aggregates. For DLCA d_f equals 1.86 whereas $d_f = 2.1$ results for the RLCA regime.²⁸ The number of particles in an aggregate N is related to the radius of gyration R_g of the aggregates and single particle radius a as²²

$$N = (R_g/a)^{d_f} \quad (1)$$

In the case of the DLCA, von Smoluchowski³⁰ has shown that the Brownian aggregation time t_p is related to the aggregate number concentration C at time t and the initial particle concentration C_0 :

$$\frac{C_0}{C(t)} = 1 + \frac{k_{11}}{2W} C_0 t = 1 + \frac{t}{t_p} \quad (2)$$

The initial particle concentration can be calculated using the particle volume fraction Φ and the initial particle radius a with $C_0 = 3\Phi/4\pi a^3$. Here t_p is the Brownian aggregation time and W is the stability ratio given by the ratio of the coagulation rate constant k_{11} in the limit of the DLCA to the rate constant measured in case of the RLCA.^{24,25} The coagulation rate constant for binary collisions in the DLCA regime results to $k_{11} = 8k_B T/3\eta$, where $k_B T$ denotes the thermal energy of the particles and η the viscosity of the solvent. Approximating k_{11} in eq 4 by the von Smoluchowski rate constant $k_{11,Sm}$ and substituting C_0 yields a theoretical Brownian aggregation time $t_p = \eta \pi R_{h,0}^3 W / \Phi k_B T$. Combining eq 1 and 2, one gets for the average size \bar{R}_g in the limit of long aggregation times ($t/t_p \gg 1$)^{22,27}

$$\bar{R}_g/a = (1+t/t_p)^{1/d_f} \approx (t/t_p)^{1/d_f} \quad (3)$$

In what is to follow, the average size of the particles and the aggregates will be measured by DLS. Thus, we approximate a as the initial hydrodynamic radius $R_{h,0}$ of the dissolved polymers. Moreover, the size of the polydisperse aggregates \bar{R}_g must now be replaced by their hydrodynamic radius $R_h(t)$. In principle, this step requires precise knowledge about the size distribution of the aggregates. Since the present experiments are conducted practically in the limit of the DLCA or near to this limit, the relationship between

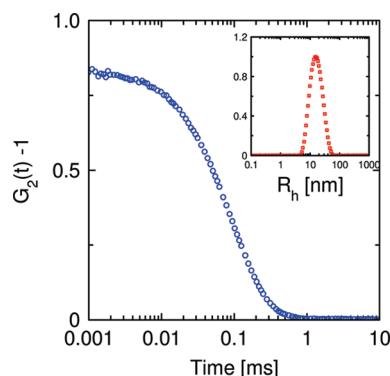


Figure 2. Intensity auto correlation function measured at 25 °C and 90° angle. The inset shows the particle size distribution calculated by using a CONTIN fit.

the radius of gyration and the hydrodynamic radius can be calculated³¹ and used for the evaluation of the DLS data:²²

$$\frac{R_h(t)}{R_{h,0}} \approx 1.129 \left(\frac{t}{t_p} \right)^{1/d_f} \quad (4)$$

whereas $R_h(t)$ is the hydrodynamic radius at time t and $R_{h,0}$ the initial particle hydrodynamic radius at time $t = 0$.

The foregoing approach suggests the following experiments: For a given polymer concentration, the analysis of the aggregation can be done by precise measurements of the hydrodynamic radius R_h as the function of time at a given temperature T . In the limit of DLCA the ratio of $R_h/R_{h,0}$ as the function of aggregation time t reduced by the Brownian aggregation time t_p should be given by a power law as stated in eq 3.²² Following the prescription of Wagner et al.,²² a master curve can be constructed by plotting $R_h/R_{h,0}$ as a function of t/t_p . We therefore determine first the temperature in which the limit of the DLCA is reached. Here, W is unity at all temperatures, and the theoretical Brownian aggregation time simplifies to $t_{p,\text{fast}} = \eta \pi R_{h,0}^3 / \Phi k_B T$. Now the dimensionless stability parameter W for the temperatures in the RLCA regime is obtained by shifting the curves in the slow coagulation regime until they overlap with the curves measured for the diffusion-limited case. Thus, $t_p = \eta \pi R_{h,0}^3 W / \Phi k_B T$ in this case or $t_p = W t_{p,\text{fast}}$. In this way W provides a measure for slowing down of the coagulation rate.

Results and Discussion

Dilute solutions containing 0.016 wt % of the dendronized polymer **PG2** were analyzed by dynamic light scattering at a temperature of 25 °C. Figure 2 shows the normalized intensity autocorrelation function measured at a scattering angle of 90°. The hydrodynamic radius was calculated using the Stokes–Einstein relation, and the particle size distribution was determined using the CONTIN program. The inset of this figure shows the particle size distribution with an average hydrodynamic radius of 18 nm.

Using the relative width of the peak the polydispersity of the particles was estimated to 1.2. Figure 2 therefore demonstrates that there is no association of polymer chains at lower temperatures, and the aggregation starts from a well-defined solution state, that is, from single molecules.

This result is supported by cryogenic transmission electron microscopy (cryo-TEM) which allows us to study the size and the possible association of the polymers and colloids in solution, that is, *in situ*.^{23,32,33} Figure 3 shows cryo-TEM images of the dendronized polymer solutions taken at temperatures of 25 and 60 °C. Figure 3a, which has been taken at room temperature,

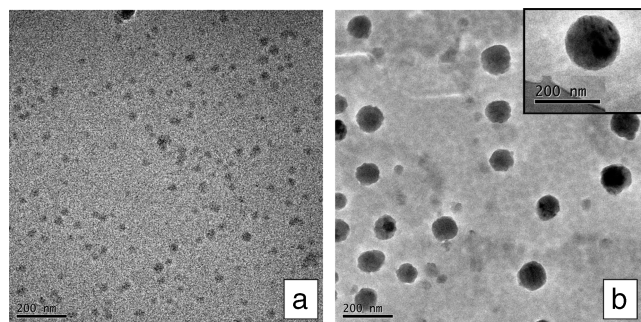


Figure 3. Cryo-TEM images of the dendronized polymer at different temperatures. (a) Image taken at a solution temperature of 25 °C. The individual dendronized polymers are clearly visible. (b) At 60 °C the dendronized polymer chains aggregate and form stable spherical mesoglobules. The inset shows the individual single mesoglobule.

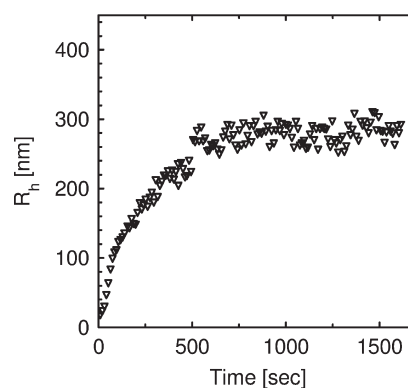


Figure 4. Hydrodynamic radius of the dendronized polymer after a sudden raise of the temperature from 25 to 35.3 °C (heating rate: 1 °C/min) using a polymer solution with a concentration of 0.016 wt %.

suggests that virtually no association takes place under these conditions. The diameter of the dendronized polymers is 35 ± 5 nm and thus compares well to the size determined by DLS. It is remarkable that the single polymer chains assume a more or less globular structure even in the fully dispersed state. This finding points to a rather small persistence length of these dendronized polymers.

Figure 3b shows a cryo-TEM image of the same solution heated to 60 °C within 10 min. The formation of the spherically shaped, stable mesoglobules at 60 °C is clearly visible. The size of the mesoglobules is 220 ± 15 nm. The inset of Figure 3b shows the close-up image of one individual mesoglobule. It clearly confirms the almost spherical shape at 60 °C. Moreover, close inspection of these globules reveals that they consist of small spherical objects that have been precipitated on their surface. Thus, cryo-TEM suggests that the mesoglobules have been generated by aggregation of small spherical objects.

Figure 3b shows two further points to be discussed in the sequel: (i) The mesoglobules exhibit a rather narrow size distribution. If the aggregation would have occurred at random, a most probable distribution should have resulted which is much broader than the breadth distribution that can be estimated from Figure 3b. (ii) The volume fraction of the mesoglobules is quite high, but no aggregation of the globules occurs anymore. Thus, the stability of the mesoglobules cannot be traced back to the slowing down of coagulation by a sufficiently small concentration.

In order to elucidate the formation of mesoglobules in further detail, the hydrodynamic radius of the **PG2** polymer and the resulting mesoglobules was determined by dynamic light scattering while raising the temperature in a well-defined fashion.

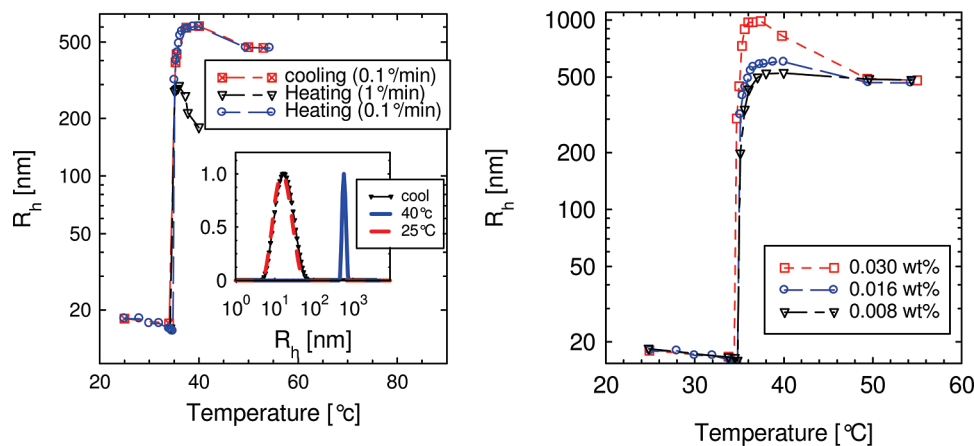


Figure 5. (a) Hydrodynamic radius R_h of the **PG2** as a function of temperature. The solution (0.016 wt %) was heated from 20 °C to the temperature indicated in the graph. The hydrodynamic radii were measured after equilibrium had been reached at each temperature. Heating and cooling was done using rates of 0.1 and 1 °C/min, respectively. The inset shows the corresponding particles size distributions at the heating and cooling rate of 0.1 °C/min calculated from CONTIN fits at 25 and 40 °C and again at 25 °C after cooling to the respective temperature. (b) Change of hydrodynamic radius with temperature at three different polymer concentrations.

Cryo-TEM has shown that the monomeric **PG2** as well as the mesoglobules are spherical. Therefore, the hydrodynamic radius leads directly to the size of the object as the function of temperature. Figure 4 displays the increase of the hydrodynamic radius with time if the sample is heated with a heating rate of 1 °C/min from 25 to 35.3 °C. There is a strong increase of R_h which points to the rapid formation of aggregates. However, R_h levels off after ca. 1000 s, and a plateau value is reached. This situation remains stable for hours. It demonstrates that the polymer under consideration here forms well-defined mesoglobules in the size range of ~ 300 nm in radius. This is in qualitative agreement with the micrographs obtained under similar conditions by cryo-TEM (Figure 3). A quantitative agreement cannot be expected since the size of the mesoglobule depends on the heating rate (see below).

Figure 5 shows the hydrodynamic radius of the dendronized polymer in equilibrated states during several heating and cooling cycles. The solution was first heated slowly with a rate of 0.1 °C/min starting from 24 °C until the temperature of 34.9 °C was reached. First, the chains shrink as indicated by the small change in the hydrodynamic radius from 18 to 16 nm, as shown in Figure 5a. This is to be expected because the solvent quality decreases slowly when going from 24 to 34.9 °C. However, a further raise of the solution temperature to 35 °C results in a sudden increase of the hydrodynamic radius of the polymer particles to ~ 317 nm. This state is found to be stable and may thus be regarded as a local equilibrium. The temperature was then raised further in small steps (0.3 °C) which resulted in even larger aggregates. Each state corresponds to a stable mesoglobule at the given temperature. Finally, between 38 and 40 °C the aggregates reach a hydrodynamic radius of 600 nm, which remains constant up to 50 °C. Raising the temperature further, the mesoglobules are found to shrink to well-defined, nearly monodisperse aggregates of ~ 450 nm, shown in the inset of Figure 5a.

Cooling runs were performed in the same way. The temperature was decreased at a rate of 0.1 °C/min to the given temperature and then kept constant until a stable state of the aggregates was reached again. The cooling process was interrupted at the same temperatures adjusted in the heating process before. In this way the measured hydrodynamic radii R_h obtained for heating and cooling runs could directly be compared. R_h was found to depend hardly on the direction in which the temperature was reached. The heating/cooling cycles were repeated several times leading always to the same results. The heating experiment was repeated by using a higher heating rate of 1 °C/min. The triangles

in Figure 5a indicate that again well-defined aggregates were formed the size of which, however, was smaller than the size obtained at a slower heating rate (0.1 °C/min).

Figure 5 hence demonstrates that there is virtually no hysteresis between the cooling and heating process. This finding is remarkable since considerable hysteresis is commonly observed for other systems: Kujawa et al., e.g., found a marked hysteresis for mesoglobules formed by poly(*N*-isopropylacrylamide).⁵ Also, Cheng et al. studying the association and dissociation of the same polymer in aqueous solution reported similar findings.⁷ They explained the hysteresis by assuming additional hydrogen bonds between the densely packed chains in the globule. Such additional bonds resemble cross-linking points that render the globules more stable against dissociation. Recently, Wu and co-workers found that poly(*N,N*-diethylacrylamide) (PDAAEM) changes from the coiled to single-chain globule state without any hysteresis in the cooling and heating cycles.³⁴ The authors state that this finding is due to the lack of intrachain hydrogen bonding in the single-chain globules. The absence of a hysteresis for the present system thus points to the absence of strong hydrogen bonding within the mesoglobule, which is in agreement with the polymer's chemical structure lacking any site capable of hydrogen bond formation.

The apparent lower critical solution temperature (LCST) depends only slightly on concentration. Figure 5b shows the change of the hydrodynamic radius as a function of temperature depending on the concentration of the solution. For more highly concentrated solutions, increasingly larger aggregates are formed which at ~ 50 °C merge to a globules of a size of ~ 500 nm. In the present system the formation of stable mesoglobules of similar sizes seems to be a robust phenomenon that does not depend strongly on concentration.

In order to further estimate the conformation of the mesoglobules the ratio of R_g/R_h has been calculated. The value of the radius of gyration R_g was determined by performing additional static light scattering measurements. The static light scattering intensities were measured at scattering angles between 30° and 130° with an angular step of 10°. The R_g values are calculated by using Guinier's approach. At room temperature the individual dendronized polymer has a radius of gyration of 22 nm and a hydrodynamic radius of 18 nm, resulting in a ratio $R_g/R_h \sim 1.2$. This ratio corresponds to flexible coiled chains.⁴ A further increase in the temperature from 25 to 40 °C with a heating rate of 1 °C/min gives rise to a decrease of R_g/R_h from 1.2 to ~ 0.7 . A uniform sphere has the R_g/R_h of 0.7744.³⁵ Thus, these results

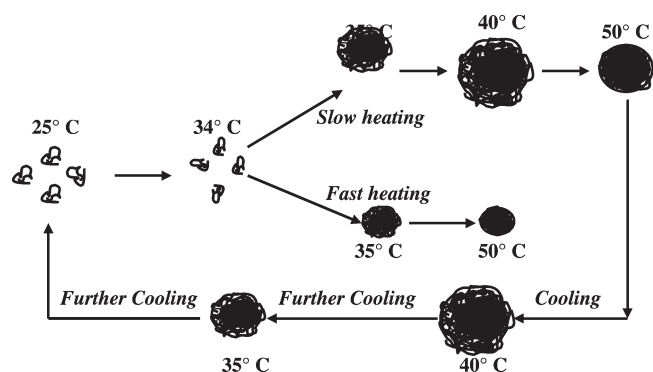


Figure 6. Schematic representation of temperature-dependent PG2 association and dissociation at different heating and cooling cycles using two different heating rates (slow: 0.1 °C/min; fast: 1 °C/min). The PG2 chains shrink up to 34 °C. Then mesoglobule formation starts at the LCST of 35 °C. During the cooling cycle, the mesoglobules completely disaggregate back into individual polymer chains.

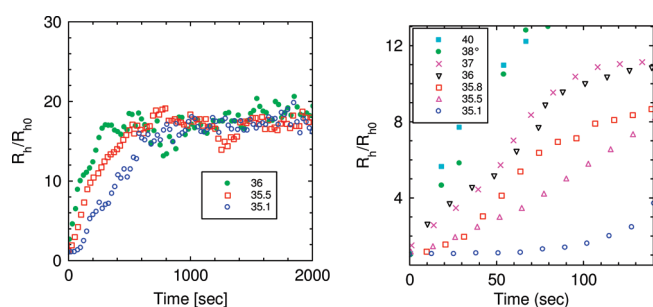


Figure 7. (a) Change in the hydrodynamic radius normalized with its initial radius as a function of the time for the dendronized polymer at different temperature conditions (heating rate: 1 °C/min). The concentration of the polymer was 0.016 wt %. (b) Change in the hydrodynamic radius normalized with its initial radius at the early time scale.

confirm the spherical shape of the mesoglobules in agreement with the cryo-TEM micrographs shown in Figure 3.

Figure 6 displays a schematic model of the association and dissociation of PG2. The chains contract until the LCST of 35 °C is reached. Exactly at this temperature the formation of mesoglobules starts. The size of the stable mesoglobules depends on the heating rate. At even higher temperatures the nearly monodisperse mesoglobules that have been formed slightly shrink but remain stable. The mesoglobules formed at a slow heating rate (0.1 °C/min) are larger than the ones formed at a fast heating rate (1 °C). During the cooling cycle the mesoglobules completely dissociate back into individual polymer chains as is evident from Figure 4a. Moreover, virtually no hysteresis is found when comparing the cooling runs to the heating runs.

In order to investigate the formation of mesoglobules of PG2 in solution in detail, the kinetics of aggregation at different temperatures was analyzed quantitatively. The analysis of the aggregation as the function of temperature was done at a low polymer concentration (0.016 wt %). First, the hydrodynamic radius $R_h(t)$ is normalized to its initial value $R_{h,0}$ at time $t = 0$ for different temperatures. Figure 7a displays $R_h(t)/R_{h,0}$ as a function of time obtained from DLS at different temperatures. For the sake of clarity, only data for three different temperatures are shown. Obviously, $R_h(t)/R_{h,0}$ is rapidly increasing above the value of 1.38 resulting for dimers.^{25,26} Figure 7b focuses on the early time scale and shows that the dependence of $R_h(t)$ on time t differs markedly with increasing temperature. For high temperatures the rate of mesoglobule formation is much faster compared to low temperatures. In particular, Figure 7 demonstrates that the rate of mesoglobule formation does not increase anymore when

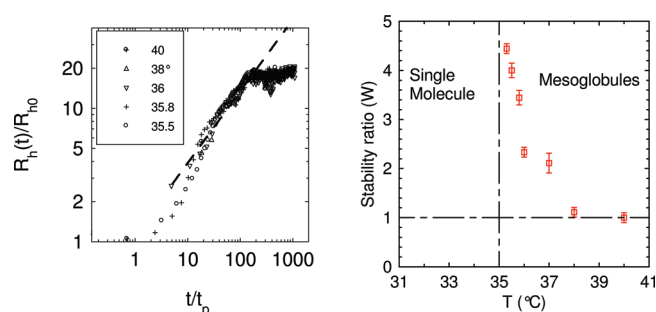


Figure 8. (a) Master curve of the intermediate stage of aggregation: Here the data presented in Figure 6 are plotted according to eq 4. The dashed line corresponds to the fractal dimension of the aggregates with $d_f = 1.89$. The parameter $t_p = \eta \pi R_{h,0}^3 W / \Phi k_B T$ contains the stability ratio W which is used as a fit parameter here. W is chosen so that the curves overlap in the intermediate regime of t/t_p . (b) The stability ratio W is thus determined as the function of the temperature T . Three regimes can be discerned: For temperatures below 35 °C, single chains are stable in solution. For temperatures 35 °C < T < 38 °C there is a cluster–cluster aggregation following the RLCA. Finally, above 38 °C the monomers and small clusters are unstable in the intermediate stage and their aggregation follows the DLCA.

going from 38 to 40 °C. From this observation we conclude that the diffusion-limited colloidal aggregation for the present system is reached at 38 °C. Hence, there must be a finite repulsion between the polymers or the clusters that only vanishes at 38 °C and above. In principle, the observations shown in Figure 7b clearly demonstrate that there is a transition from the RLCA to the DLCA at 38 °C which should be followed by a different fractal dimension d_f (see above) and a stability ratio $W > 1$. However, the present limits of error do not allow us to analyze a small change of the exponent. Hence, in what is to follow we give a simplified treatment in terms of the DLCA only.

In order to apply the analysis of Borkovec and co-workers,²⁶ aggregation must be restricted to the very early stage of aggregation where mostly dimers are formed. Hence, $R_h(t)/R_{h,0}$ should not exceed the value of 1.38 in the DLS experiments.^{25,26} However, these conditions cannot be reached for the present system as shown in Figure 7. As mentioned above, the DLS measurements of the present system require a certain minimum concentration which is beyond this regime and the evaluation of the data (Figure 7) will be given in terms of the approach of Wagner et al.²² It must be kept in mind that the theory of ref 22 was developed for a system of hard spheres that aggregate to a fractal network. The cryo-TEM micrographs in Figure 3, on the other hand, indicate that the final stage of the aggregation of PG2 is given by spherical mesoglobules. Thus, we restrict the analysis along these lines to the early stage and apply it on a semiquantitative level only.

The Brownian aggregation time of the aggregates t_p can be determined out of $R_h(t)/R_{h,0}$ at different temperatures according to eq 3. As discussed above, the stability ratio W is used as a fit parameter and chosen so that a master curve for all measurements of $R_h(t)/R_{h,0}$ in the intermediate stage results (see Figure 8a): For $t/t_p \leq 10$ the data points do not fit on the master curve since in this early stage single polymer chains begin to merge into clusters. At $10 \leq t/t_p \leq 100$, however, all data points measured at different temperatures fall onto one master curve. Obviously, the mesoglobule formation can be described in this intermediate stage by the approach devised by Wagner et al.²² The slope of the dashed line in Figure 8a is related to the fractal dimension of the aggregates d_f . The slope is compatible with the established value 1.86 for the DLCA. However, the present limits of error and the various approximation involved in this evaluation do not allow a more precise determination of the exponent from the present experimental data.

Beyond $t/t_p \geq 100$, however, the growth rate of the aggregates rapidly slows down as the mesoglobules become stable. In contrast to the situation encountered in the coagulation of destabilized colloidal particles,^{25,26,22} aggregation comes to an end if a given size of the mesoglobules is reached. The reasons for this sudden change from aggregation to stable mesoglobules will be discussed further below.

All results can be resumed in a state diagram given in Figure 8b (cf. also Figure 3 of ref 4). Plotting the dimensionless stability ratio W as a function of the solution temperature T clearly reveals three regimes: Below 35 °C **PG2** forms stable solutions in water. Above this temperature two coagulation regimes (Figure 8b) can be discerned. For temperatures between 35 and 38 °C W is found to decrease with increasing temperature. For temperatures $T \geq 38$ °C we find that the curves $R_h(t)/R_{h,0}$ as the function of t/t_p do not change upon further raise of T . Hence, $W = 1$ and the diffusion-limited coagulation regime is reached. The temperature that separates the fast from the slow aggregation regime may be regarded as the critical aggregation temperature of the dendronized polymer. In the case of **PG2**, we find the critical aggregation temperature at ~ 38 °C. Above this temperature the monomeric chains and small clusters thereof have become totally unstable. Only mesoglobules of a certain size that result for $t/t_p > 200$ are stable against further coagulation.

It rests to discuss possible reasons for the sudden stop of aggregation which is obvious from the DLS experiments and the cryo-TEM micrographs. Figure 8a shows this feature in a most marked way: $R_h/R_{h,0}$ increases as expected for a system of coagulating spheres.²² However, at $t/t_p \approx 200$, the growth of the mesoglobules stop and no further aggregation takes place. In particular, no Ostwald ripening of the globules is found that would lead to a broad size distribution, but the resulting objects are rather narrowly dispersed (see Figure 3). The reasons for the stability of mesoglobules in solution have been comprehensively discussed by Winnik and co-workers.⁴ First of all, steric stabilization can be invoked when dealing with amphiphilic polymers.^{8,36} Another mechanism leading to stabilization must be sought in the viscoelastic effect first proposed by Wu and co-workers.³ The mesoglobules are partially vitrified which may render the mutual collisions ineffective. Electrostatic stabilization by small amounts of ions immobilized in the mesoglobules may provide another mechanism for stability.^{37,38}

It is interesting to note that the temperature of the maximum size of the mesoglobules coincides with the critical coagulation temperature identified above. Thus, the stability of smaller mesoglobules below this temperature must be at least partially due to a finite steric stabilization. This finite steric stabilization obviously is responsible for the well-defined size of the mesoglobules at a given temperature (see Figure 5). In this way the findings discussed in conjunction with Figure 5 can directly be compared to the state diagram Figure 8 and the stability ratio W : A stability ratio $W > 1$ results from a more effective steric stabilization that allows the system to generate more surface. Hence, smaller mesoglobules result.

However, above the critical coagulation temperature the reason for the stability of mesoglobules can hardly be sought in steric stabilization by the dendrons. Evidently, single chains are unstable and coagulate, thus indicating the absence of steric stabilization. The only stabilizing effects that may be operative under these conditions are the viscoelastic effect and the electrostatic stabilization^{5,37,38} discussed above. Electrostatic stabilization may be invoked because the dendrons attached to the main chains are similar to crown ethers known to be excellent complexation agents for small ions.³⁹ Hence, each dendronized polymer may have been complexed by a small number of ions that are kept when aggregating to larger spheres. If the charge of a given mesoglobule has become large enough, the electrostatic

stabilization has also increased to the level that the mesoglobules repel each other. At this stage no further growth takes place. A similar mechanism was recently discussed by Stradner et al. when discussing the aggregation of charged proteins.⁴⁰ This conjecture would also explain the rather narrow size distribution: a minimum size is required for obtaining the sufficient charge; smaller globules are not stable. Beyond a certain charge no further coagulation takes place.

In order to further investigate the stabilization mechanism, we performed kinetic measurements of the mesoglobule formation in presence of 0.01 mol/L sodium chloride. The DLS measurements show that at room temperature the size of the dendronized polymer chains remains constant as expected. Increasing the temperature to 35.1 °C initiates the formation of mesoglobules. In line with the salt-free experiments the mesoglobules grow until reaching a specific hydrodynamic radius of 650 nm, at which the size remains constant. However, the polydispersity of the formed mesoglobules is much higher than in salt-free conditions, and the radius is smaller. Similar results are found by raising the concentration of sodium chloride to 0.05 mol/L. The marked increase of the polydispersity points to the fact that the process of aggregation in presence of salt is not stopped anymore at a well-defined point. However, the aggregation still does not proceed to a fully macroscopic phase.³⁸ We hence conclude that the viscoelastic effect may still be operative under these conditions: If the volume fraction of the PMMA main chains of **PG2** exceeds a certain value, the globules are vitrified. Collisions between two mesoglobules thus become ineffective, and a stable suspension results.

Conclusion

We investigated the solution behavior of the thermosensitive dendronized polymer **PG2** at different temperature conditions using dynamic light scattering and cryo-TEM. At temperatures higher than the LCST of 35 °C, a coil-to-mesoglobule transition of the polymer chains in solution is observed. The resulting mesoglobules are stable and nearly monodisperse. Upon cooling, the mesoglobules completely dissociate back into singular chains without any marked hysteresis. In dilute concentrations the equilibrium size of the mesoglobules is a function of the solution temperature. Also, the equilibrium size of the aggregates in high temperature conditions above 50 °C weakly depends on the polymer concentration. We showed that the intermediate stage of the formation of mesoglobules can approximately be described by a cluster-cluster aggregation model as devised by Wagner and co-workers.²² The master curve (see the discussion of eq 4) exhibits three different stages during the formation of mesoglobules: In a first stage single chains aggregate to form clusters. In the intermediate regime ($5 \leq t/t_p \leq 100$), these clusters aggregate.²² Finally, aggregation stops when the mesoglobules have reached a certain size. Possible reasons for the stability of the globules of a certain size may be sought in an electrostatic stabilization originating from complexed stray ions,^{5,37} most probably supported by a finite viscoelastic stabilization.³

Acknowledgment. Financial support by the Deutsche Forschungsgemeinschaft, SFB 481, Bayreuth, the ETH Research Grant ETH-1608-1, and the National Natural Science Foundation of China (Nos. 20374047 and 20575062) is gratefully acknowledged. C.S. gratefully acknowledges the support of the Elite Network of Bavaria ENB.

References and Notes

- (1) Flory, P. J. *Principles of Polymer Chemistry*; Cornell University Press: Ithaca, NY, 1953.
- (2) Siu, M.; Liu, H. Y.; Zhu, X. X.; Wu, C. *Macromolecules* **2003**, *36*, 2103.

- (3) Wu, C.; Li, W.; Zhu, X. X. *Macromolecules* **2004**, *37*, 4989.
- (4) Chen, H.; Zhang, Q.; Li, J.; Ding, Y.; Zhang, G.; Wu, C. *Macromolecules* **2005**, *38*, 8045.
- (5) Kujawa, P.; Aseyev, V.; Tenhu, H.; Winnik, F. M. *Macromolecules* **2006**, *39*, 7686.
- (6) Kujawa, P.; Tanaka, F.; Winnik, F. M. *Macromolecules* **2006**, *39*, 3048.
- (7) Cheng, H.; Shen, L.; Wu, C. *Macromolecules* **2006**, *39*, 2325.
- (8) Zhang, Q.; Ye, J.; Lu, Y.; Nie, Y.; Xie, D.; Song, Q.; Chen, H.; Zhang, Q.; Tang, Y.; Wu, C.; Xie, Z. *Macromolecules* **2008**, *41*, 2228.
- (9) Wu, C.; Zhou, S. Q. *Macromolecules* **1995**, *28*, 5388.
- (10) Wang, X.; Qiu, X.; Wu, C. *Macromolecules* **1998**, *31*, 2972.
- (11) Nakata, M.; Nakumara, Y.; Sasaki, N.; Maki, Y. *Phys. Rev. E* **2007**, *76*, 041805.
- (12) Ding, Y. W.; Ye, X. D.; Zhang, G. Z. *Macromolecules* **2005**, *38*, 904.
- (13) Picarra, S.; Gomes, P. T.; Martinho, J. M. G. *Macromolecules* **2000**, *33*, 3947.
- (14) Maeda, Y.; Nakamura, T.; Ikeda, I. *Macromolecules* **2001**, *34*, 1391.
- (15) Kjoniksen, A. L.; Zhu, K.; Pamies, R.; Nyström, B. *J. Phys. Chem. B* **2008**, *112*, 3294.
- (16) Byrne, A.; Kiernan, P.; Green, D.; Dawson, K. A. *J. Chem. Phys.* **1995**, *102*, 573.
- (17) Kuznetsov, Y. A.; Timoshenko, E. G.; Dawson, K. A. *J. Chem. Phys.* **1996**, *104*, 3338.
- (18) Ye, X.; Lu, Y.; Shen, L.; Ding, Y.; Liu, S.; Zhang, G.; Wu, C. *Macromolecules* **2007**, *40*, 4750.
- (19) Xu, J.; Zhu, Z. Y.; Luo, S. Z.; Wu, C.; Liu, S. Y. *Phys. Rev. Lett.* **2006**, *96*, 027802.
- (20) Chu, B.; Ying, Q. *Macromolecules* **1996**, *29*, 1824.
- (21) Li, W.; Zhang, A.; Schlüter, A. D. *Chem. Commun.* **2008**, 5523–5525.
- (22) Hanus, L. H.; Hartzler, R. U.; Wagner, N. J. *Langmuir* **2001**, *17*, 3136.
- (23) Wittemann, A.; Drechsler, M.; Talmon, Y.; Ballauff, M. *J. Am. Chem. Soc.* **2005**, *127*, 9688.
- (24) Evans, D. F.; Wennerström, H. *The Colloidal Domain*; Wiley-VCH: Berlin, 1999.
- (25) Holthoff, H.; Egelhaaf, S. U.; Borkovec, M.; Schurtenberger, P.; Sticher, H. *Langmuir* **1996**, *12*, 5541.
- (26) Holthoff, H.; Schmitt, A.; Fernandez, B. A.; Borkovec, M.; Cabrerizo, V.; Miguel, A.; Schurtenberger, P.; Hidalgo, A. R. *J. Colloid Interface Sci.* **1997**, *192*, 463.
- (27) Lin, M. Y.; Lindsay, H. M.; Weitz, D. A.; Ball, R. C.; Klein, R.; Meakin, P. *Nature* **1989**, *339*, 360.
- (28) Lin, M. Y.; Lindsay, H. M.; Weitz, D. A.; Klein, R.; Ball, R. C.; Meakin, P. *J. Phys.: Condens. Matter* **1990**, *2*, 3093.
- (29) Lin, M. Y.; Lindsay, H. M.; Weitz, D. A.; Ball, R. C.; Klein, R.; Meakin, P. *Phys. Rev. A* **1990**, *41*, 2005.
- (30) von Smoluchowski, M. *Phys. Z.* **1916**, *17*, 557.
- (31) Torres, F. E.; Russel, W. B.; Schowalter, W. R. *J. Colloid Interface Sci.* **1991**, *142*, 554.
- (32) Crassous, J.; Wittemann, A.; Siebenbürger, M.; Schrunner, M.; Drechsler, M.; Ballauff, M. *Colloid Polym. Sci.* **2008**, *286*, 805.
- (33) Crassous, J.; Drechsler, M.; Ballauff, M.; Schmidt, J.; Talmon, Y. *Langmuir* **2006**, *22*, 2403.
- (34) Zhou, K.; Lu, Y.; Li, J.; Shen, L.; Zhang, G.; Xie, Z.; Wu, C. *Macromolecules* **2008**, *41*, 8927.
- (35) Aseyev, V.; Hietala, S.; Laukkanen, A.; Nuopponen, M.; Confortini, O.; Prez, F. E. D.; Tenhu, H. *Polymer* **2005**, *46*, 7118.
- (36) Vasilevskaya, V.; Khalatur, P. G.; Khkhlov, A. R. *Macromolecules* **2003**, *36*, 10103.
- (37) Chan, K.; Pelton, R.; Zhang, J. *Langmuir* **1999**, *15*, 4018.
- (38) Balu, C.; Delsanti, M.; Guenou, P.; Monti, F.; Cloitre, M. *Langmuir* **2007**, *23*, 2404.
- (39) For example, see: Buschmann, H.-J.; Mutihac, R.-C.; Schollmeyer, E. *J. Solution Chem.* **2009**, *38*, 209–217, and references cited therein.
- (40) Stradner, A.; Sedgwick, H.; Cardinaux, F.; Poon, W. C. K.; Egelhaaf, S. U.; Schurtenberger, P. *Nature* **2004**, *432*, 492.